A JOINT WITH TUNABLE COMPLIANCE FOR A CHANGE OF LOCOMOTION PATTERNS

Max Fremerey[1] and Hartmut Witte[1]

[1]Technische Universität Ilmenau, Chair of Biomechatronics, 98693 Ilmenau, Germany
{maximilian-otto.fremerey, hartmut.witte}@tu-ilmenau.de

ABSTRACT

This paper introduces a joint with active tunable compliance in order to change locomotion patterns of mobile, bio-inspired robots. Using a spring off the shelf with linear stiffness coefficient, a change in joint compliance is realized by changing relevant lever lengths inside the joint. Thereby the design follows VDI 2206, the design guideline for mechatronic products. Based on a mathematical calculation as well as on a multi-body-simulation inside SOLIDWORKS MOTION a first prototype was manufactured and tested. Comparison of measured data with those values theoretically predicted entails the design and production of the JWTC 2.0. By implementing the mechanism inside the underactuated swimming robot URMELE the authors intend to change locomotion patterns in a defined and reproducible manner.

Index Terms – Compliant actuator, active tunable compliance, swimming robot

1. INTRODUCTION AND MOTIVATION

Interpreting compliant elements in animals Cavagna et al. 1977 postulated the spring-mass interaction as one of the 'two basic mechanisms for minimizing energy expenditure' [2] in terrestrial locomotion. The first calculus for spring-mass models was introduced in 1986 by Blickhan (published in 1989), making the effects of compliance mathematically manageable [1]. In later years, he and his co-workers (Wagner, Seyfarth, Geyer) illustrated the importance of compliant elements for self-stabilization of pedal locomotion under the term 'robustness'. Thus 'intelligent mechanics' (Witte & Fischer, SAB '98) allows to avoid (or at least to reduce) the amount of neural resp. technical calculation for control purposes. Aligning these results with the requirements for mobile robots, directed tuneable compliance in the drive chain of the robot may offer several benefits: Robust locomotion following an adaption to different substrates, due to a real-time shift between defined gaits, could be achieved as well as an optimization of the overall power requirement – with reduced control effort.
Transferring the biological principles of tuneable compliant elements to techniques is done by several groups (van Ham et al., Tonietti et al., Sugar et al.). Mainly in the research field 'compliant actuators' several prototypes were introduced, e.g. MACCEPA [7] or the 'JACK SPRING' actuator [5]. Based on these scientific findings, the authors want to provoke concerted changes in locomotion patterns of mobile robots by the use of tuneable spring elements. To allow neglection of the effects of gravitation during investigation (the dominating dynamic component during terrestrial locomotion even in fast gaits and in arboreal locomotion), the swimming robots URMELE LIGHT and URMELE [3, 4] are objects of our interest, which compensate this influence of gravity by lift in a fluid. Both robots consist of a basic module

each which hosts electronics and control as well as a single drive. This actuator drives several effector modules transferring the torque created into a propulsive motion. The connection among the effector modules is realised by yet manually changeable but tuneable tension springs. Therefore we follow our approach as it is detailed in [3] and [4].

2. IDEA OF THE JWTC

In order to change the spring stiffness between the effector modules during the operation of the robot in realtime, the JWTC is introduced (**J**oint **W**ith **T**unable **C**ompliance). Fig. 1 illustrates the working principle of the JWTC.

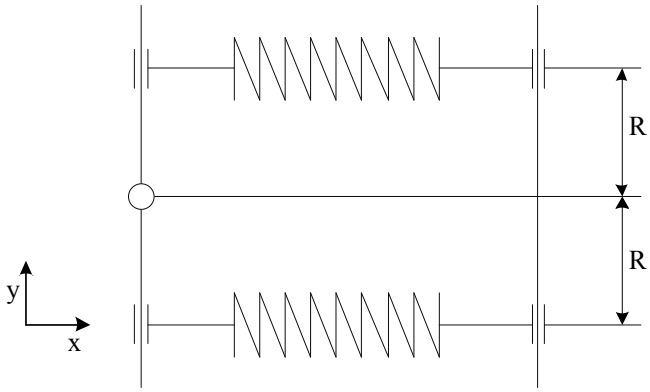

Fig. 1: working principle of the JWTC

Inspired by a design methodology according to Vanderborght et al. [6] and the requirements of the underactuated swimming robot URMELE, the joint compliance of the JWTC is affected by changing the length R which describes the distance between the center line of the revolute joint and the helical springs used. Due to symmetry reasons the JWTC consists of two linear helical springs which are arranged on both sides of the revolute joint. Linear bearings assure the movement in y-direction. Moving the helical springs overall e.g. by an actuator, the effective lever length is changed and therewith the overall joint compliance. Thus the JWTC forms an addition to other existing actuators with tunable compliance ([6]).

For calculation of the range of feasible spring stiffness subject to the linear springs chosen, a mathematical model is introduced. Fig. 2 displays all important length and values.

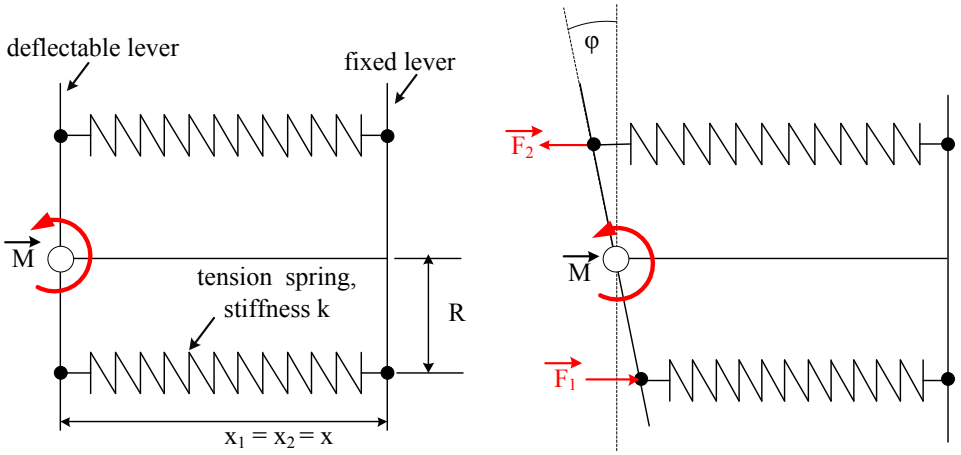

Fig. 2: model of the JWTC, M = resulting torque in Nmm, F_1, F_2 = spring forces in N, φ = excursion angle of lever in °, $x_1 = x_2 = x$= distance between fixed and mobile lever, R = changeable lever length

Thereby k marks the spring stiffness (equal for both springs) in N/mm, φ is the excursion angle of lever in °, R terms the current lever length of torque equilibrium in mm, $x_1 = x_2 = x$ describes the initial length of the springs in mm, M is the resulting torque in Nmm and F_1, F_2 are spring forces in N. Using linear helical springs, the resulting forces F_1 and F_2 amount to:

$$F_1 = (k(x - R \cdot sin(\varphi)) \qquad \text{eq. 1}$$

$$F_2 = (k(x + R \cdot sin(\varphi)) \qquad \text{eq. 2}$$

The resulting torque amounts to:

$$M = |(R \cdot (F_1 - F_2)| \qquad \text{eq. 3}$$

$$= \left|k \cdot R \cdot \cos(\varphi) \cdot [\left(x - R \cdot sin(\varphi)\right) - \left(x + R \cdot sin(\varphi)\right)]\right|$$

$$= |k \cdot R \cdot \cos(\varphi) \cdot (-2 \cdot R \cdot sin(\varphi))| \qquad \text{eq. 4}$$

By using the addition theorem

$$sin(2\varphi)) = 2\cos(\varphi) \cdot sin(\varphi))$$

eq. 4 is simplified to:

$$M = |-k \cdot R^2 \cdot sin(2\varphi))| \qquad \text{eq. 5}$$

A plot of M while varying angle φ as well as lever length R is shown in fig. 3:

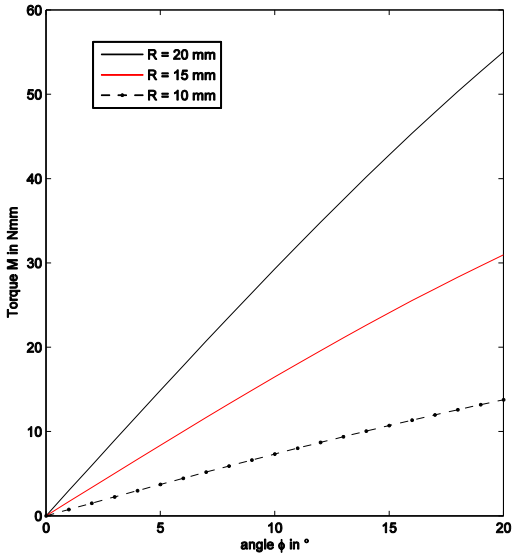

Fig. 3: calculated torque M subject to angle φ and changing lever length R

Varying R therefore enables the adjustment of different angle-torque characteristics. Following eq. 5 an increase of R raises the resulting torque.

For estimation of joint stiffness K, eq. 6 is used.

$$K = \frac{dM}{d\varphi} \qquad \text{eq. 6}$$

Considering small angles (φ < 5 °), joint stiffness K amounts:

$$K = |-k \cdot R^2 \cdot 2| \qquad \text{eq. 7}$$

For angles φ larger than 5° K equals:

$$K = |-k \cdot R^2 \cdot 2cos(2\varphi)| \qquad \text{eq. 8}$$

Fig. 4 displays the joint stiffness K subject to angle φ and lever length R.

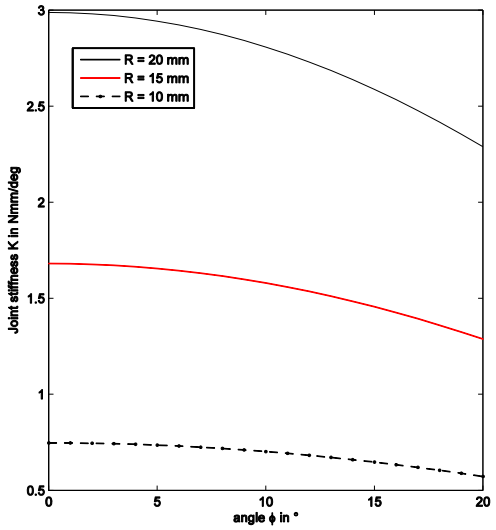

Fig. 4: joint stiffness K subject to angle φ and lever length R.

Fig. 4 illustrates the nonlinear process of the joint stiffness subject to angle φ. A change of lever length R from 10 mm to 20 mm significantly enlarges joint stiffness K: from ≈ 0,7 Nmm/deg to ≈ 3 Nmm/deg (at 0°).

In order to extend the significance of calculation done, a multi-body simulation using the multi-body tool SOLIDWORKS MOTION® is introduced. Therewith the analysis of required torque subject to spring stiffness considering geometrical properties of the joint design is possible. Fig. 5 illustrates the model used. Thereby all important lengths and parameters of the multi-body simulation like spring stiffness k, length R or angle φ mirrors the assumptions during the calculation. The results of the simulation are plotted in fig. 6. The value of spring stiffness k amounts 0.214 N/mm, the angle φ ranges between 0° and 20° due to design requirements of later applications.

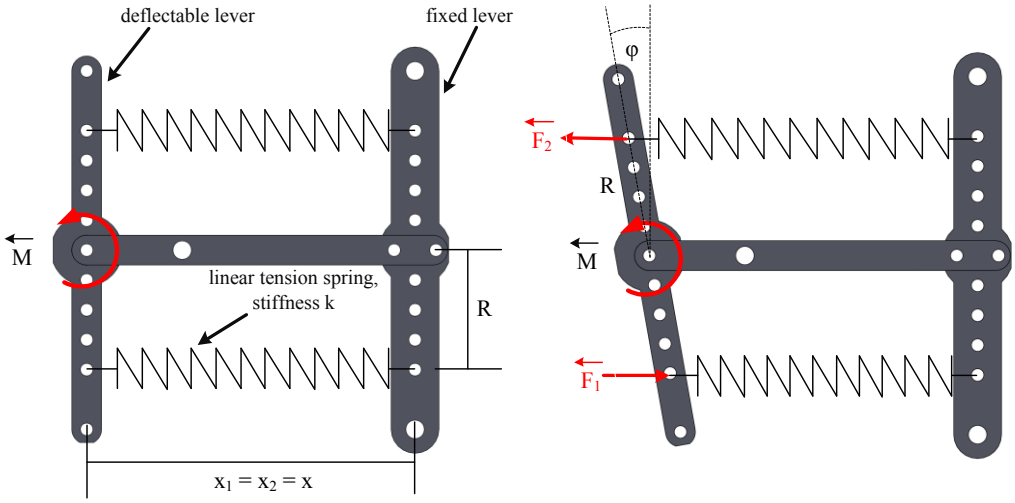

Fig. 5: model of the JWTC used for a multi-body simulation inside SOLIDWORKS MOTION, M = resulting torque in Nmm, F_1, F_2 = spring forces in N, φ = excursion angle of lever in °, $x_1 = x_2 = x$= distance between fixed and mobile lever, R = changeable lever length

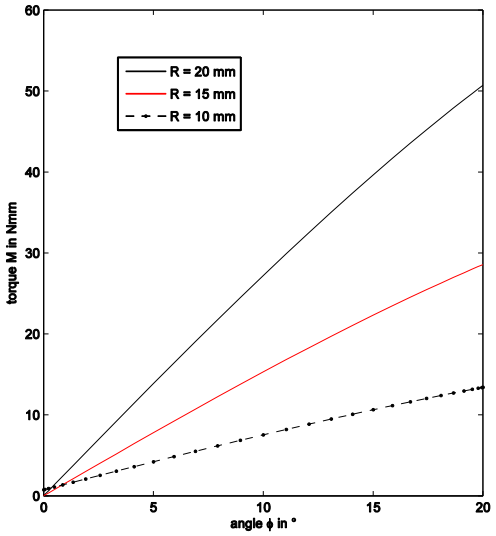

Fig. 6: calculated torque M subject to angle φ and changing lever length R inside SOLIDWORKS MOTION

Analyzing SOLIDWORKS MOTION data of rotational stiffness subject to changing lever length R confirm the results of the mathematical model: A changing lever length R influences the angle-torque characteristics. Considering gradient and point of intersection with the y-axis the plot in fig. 6 equals fig. 3.

3. EXPERIMENTS

For evaluating results of calculation and simulation, a prototype of the JWTC was designed and manufactured. Material used for design is POM (Polyoxymethylene) , the lever length enables a setting of R = 5 mm to R = 20 mm in steps of 5 mm. Spring constant k of the linear tension spring was set to 0.214 N/mm (GUTEKUNST inc.), this correlates with the value in the theoretical considerations. Fig. 7 illustrates the CAD prototype and the assembled version.

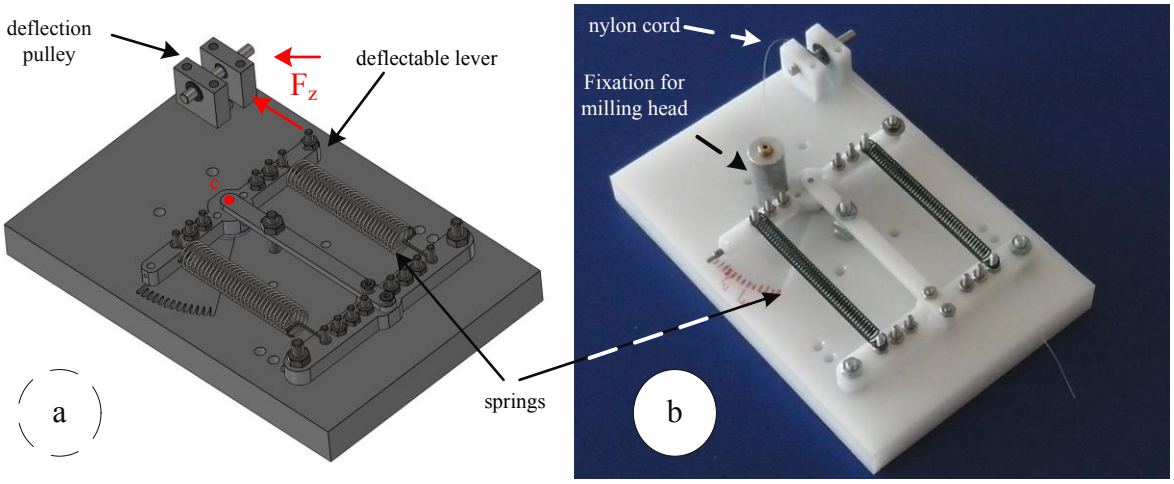

Fig 7: left: CAD prototype, **right**: assembled version of experimental setup for varying lever length R

In order to analyze the design and to compare data experiment with those from the calculation/simulation, the angle φ as well as the resulting torque M for the JWTC prototype has to be estimated. The principle of the measurement setup, a simplified pulling test, is shown in fig. 8.
By applying a force F_z from outside, this force provokes an elongation of the deflectable lever and therewith a torque around the center of the lever (red dot c in fig. 7 left). The corresponding angle φ, which is also important for proper calculation of torque M, is represented by the following relation, with respect to fig. 8 left.

$$y = h \cdot \cos\varphi \Rightarrow \cos\varphi = \frac{y}{h} \Rightarrow \varphi = cos^{-1}\frac{y}{h} \qquad \text{eq. 9}$$

with y = projected lever length due to deflection of lever in mm, h = length between center and attach point of nylon cord of deflectable lever

With a desired maximum angulation of the lever of φ = 20°, length x ranges between 0 mm (0°) and 12 mm (23.6°). The realization of the pulling test measurement setup is shown in fig. 8 right. It consists of a modified CNC milling machine moving with an accuracy of 0.03 mm in x- and y-direction and 0.02 mm in z-direction. Thereby milling head and moving lever are connected via a thin nylon cord. Moving the head with known displacement in z-direction deflects the moving lever and by using eq. 9, the resulting angle φ is calculated. The corresponding force F_z for creating the lever shifting torque is measured by a NOVATECH INC. F250UFR0H0 load cell (software used: LABVIEW® 7.5) placed between milling head and lever. Eq. 10 displays the equation for calculation of resulting torque M_R.

$$M_R = (F_Z - F_B) \cdot h \cdot \cos\varphi \qquad \text{eq. 10}$$

with M_R = resulting torque, F_z = measured force creating torque M_R with effective lever length y, F_B = offset force produced by nylon cord fixation below the load cell, h = lever length

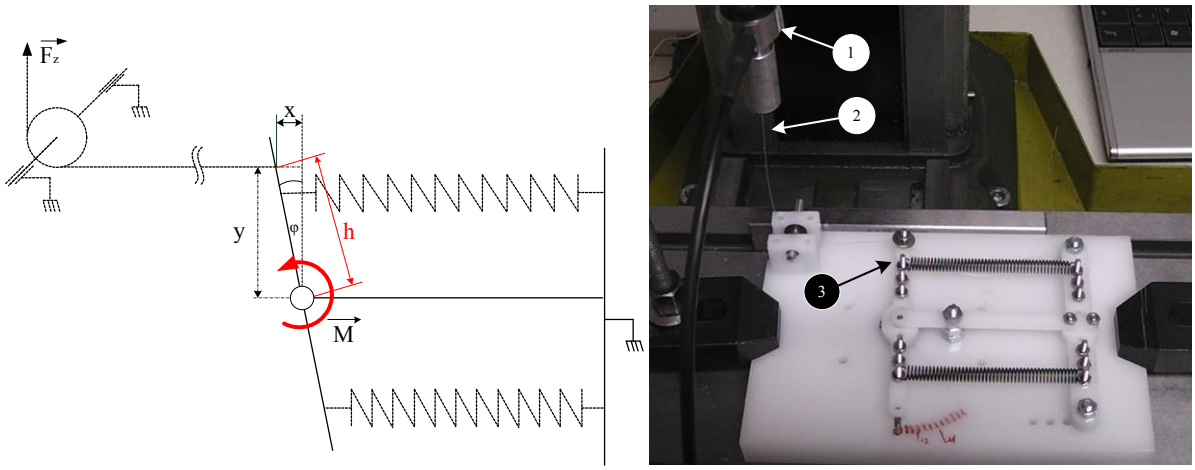

Fig. 8: left: principle of measuring characteristics of JWTC, **right:** manufactured tension-test setup (1 = force sensor, 2 = nylon cord, 3 = deflectable lever)

Considering heating period and calibration of the load cell, fig. 9 and 10 illustrates the results of experiments. Following eq. 9 and 10, fig. 9 left shows all curves having a lever length of R = 20 mm while fig. 9 right illustrates the mean value, a quadratic regression and the experimental standard deviation.

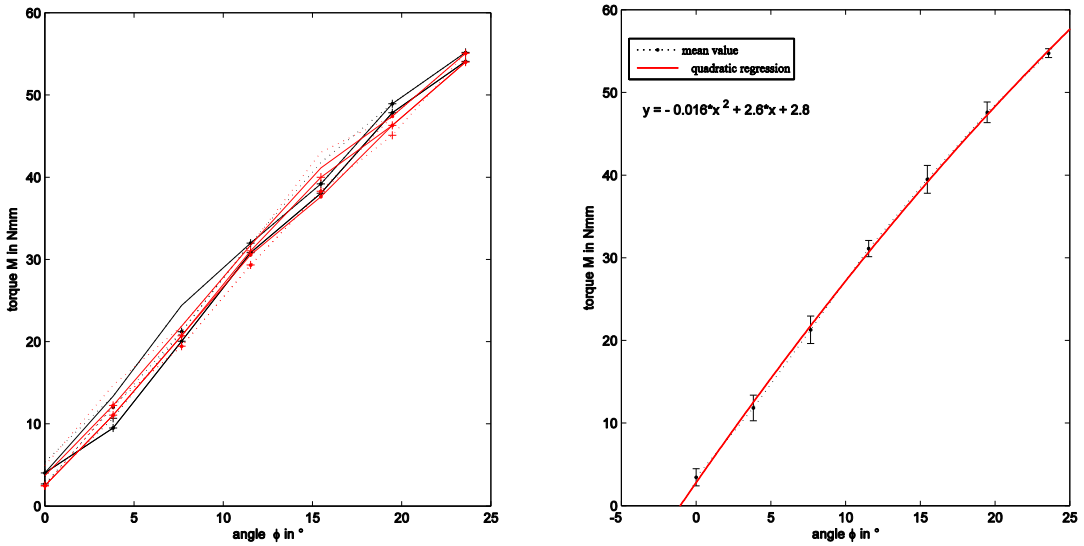

Fig. 9: left: Raw data of measured angle-torque ratio (n = 12), **right:** mean value, quadratic regression and experimental standard deviation of measured angle-torque ratio having a lever length of 20 mm

Having a lever length of R = 20 mm, the torque ranges between 2 Nmm and 4 Nmm at an angle φ of 0° and 48 Nmm to 50 Nmm at an angle φ of 20°. The course of all measurements is comparable. Matchable plot courses are also observable when analyzing the measurements (n = 12) of angle-torque relation while lever length R = 10 mm. The growth of experimental standard deviation is due to the increasing effect of friction. Having a low reset torque as a result of lever length R = 10 mm, the lever tends to stick from time to time during the measurements.

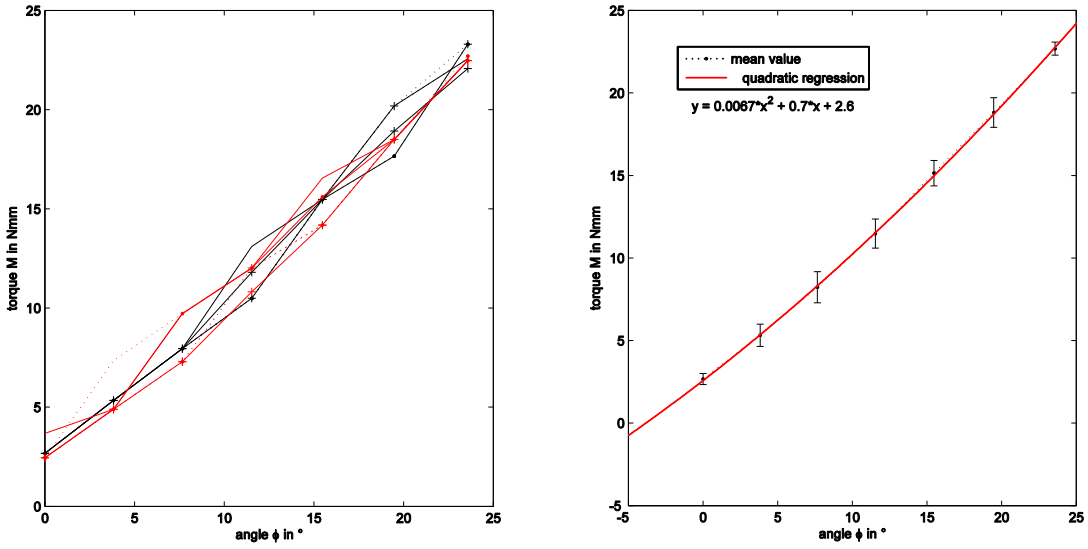

Fig 10: left: raw data of measured angle-torque ratio (n = 12), **right:** mean value, quadratic regression and experimental standard deviation of measured angle-torque ratio having a lever length of 10 mm

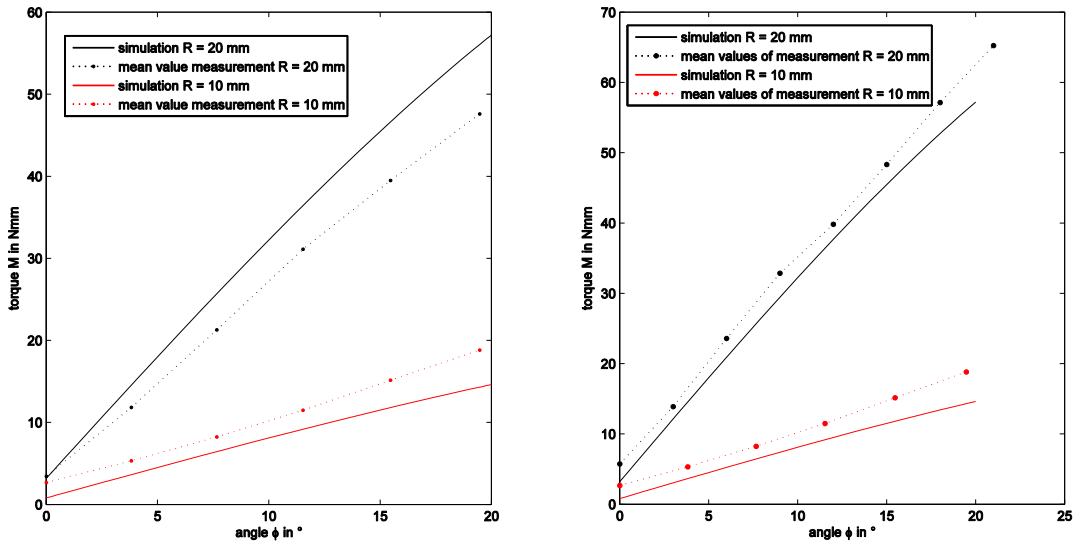

Fig 11: comparison of measurements of mean values with simulation data,
left: calculated angle φ, **right:** measured angle φ

The comparison of results of experimental mean values and simulation for R = 10 mm show the same course. Disregarding friction in theoretical consideration, the measured torque values are larger than theoretical ones. For R = 20 mm, the course of simulation and measured mean values is comparable regarding inclination. Due to manufacturing inaccuracies of elements of the measurement setup, the lever was pre-elongated even having no force F_z acting on that lever. Therewith the measurements were repeated and the elongation of the lever was estimated using the CNC-milled scale of the prototype (cp. fig. 7). The results of read off angle φ and corresponding torque are shown in fig. 11, right. Therewith the simulation predicts the course of measured mean values in a sufficient way.

However both charts in fig. 11 reveal an area where the angle-torque relationship is changeable by shifting R only.

4. DESIGN OF THE PROTOTYPE OF THE JWTC 2.0

4.1 Mechanics

Hitherto gained scientific findings and experimental results are transferred to a new version, the JWTC 2.0. The principle and a manufactured and assembled version are illustrated in fig. 12.

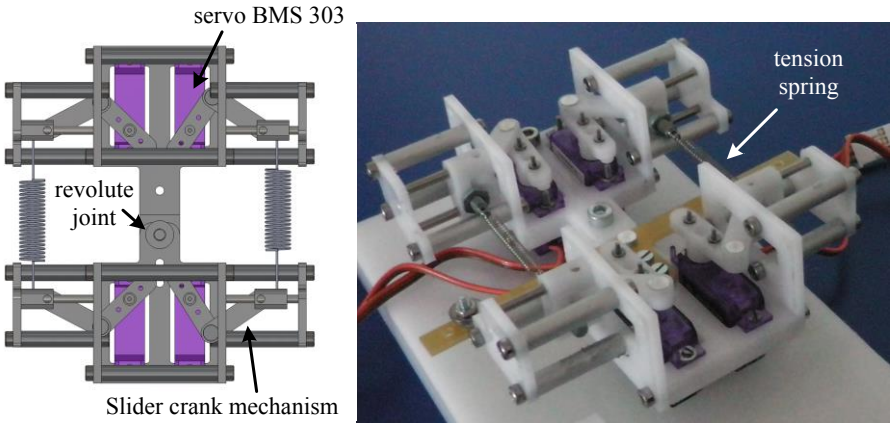

Fig. 12: CAD drawing of JWTC 2 and assembled device

The most important improvement of JWTC 2.0 is the actuation of the linear tension springs. Due to a slider crank mechanism which is driven by a servo off the shelf (BLUEBIRD BMS 303) the length R is changeable between 21.5 mm and 31.5 mm. A special shaped screw connection enables the use of different tension springs and therewith different areas of joint compliance within the same joint design. A use inside the swimming robot URMELE with its special requirements towards joint-dependent individual spring stiffness becomes feasible.

4.2 Control/Electronics and Experiments

Power for each servo is provided by an external 5V fixed voltage regulator (type 7805). During experiments, the four servo drives are controlled by an ARDUINO MEGA microcontroller-board via PWM using MATLAB SIMULINK and the ARDUINO-MATLAB plug-in. For enabling a smooth setting of the position of each of the four slider crank mechanisms subject to an individual external potentiometer, a PI controller is used (parameter P-fraction = 10, I-fraction= 1) .

During experiments, the position of the slider crank mechanism is set to the minimum position of 21.5 mm as well as to the maximum position of 31.5 mm. The spring stiffness of linear tension springs used amounts to k = 0.036 N/mm. In order to track the angle-torque relation, JWTC 2.0 is also analyzed using the pulling test setup shown in fig. 8. Length x is restricted again and ranges between 0 mm and 12 mm.
Fig. 13 and 14 illustrate the results of experiments; the area between the dotted lines in fig. 14 shows the range of adjustable angle-torque ratio and therewith joint stiffness K by varying lever length R.

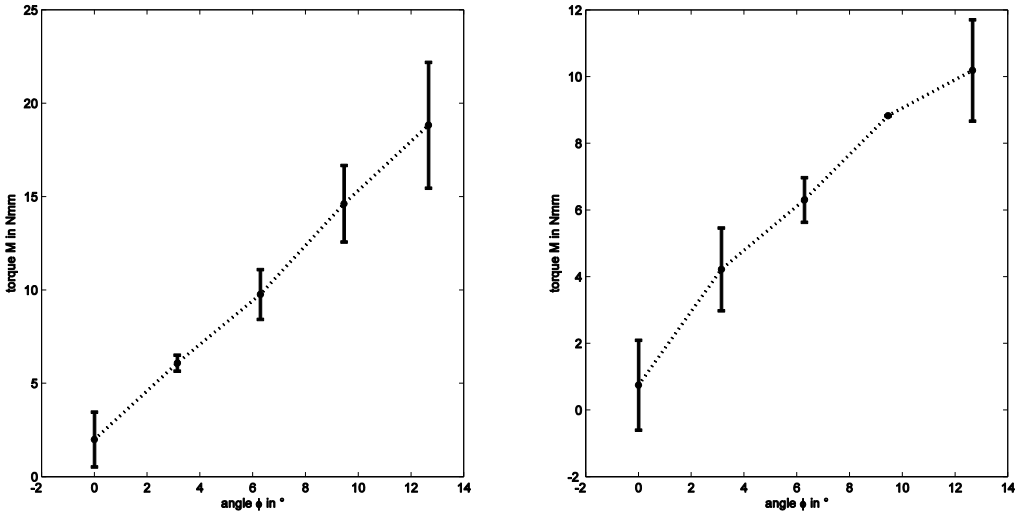

Fig. 13: mean value and experimental standard deviation for **left:** R = 21.5 mm and **right**: R = 31.5 mm; number of measurements n = 12

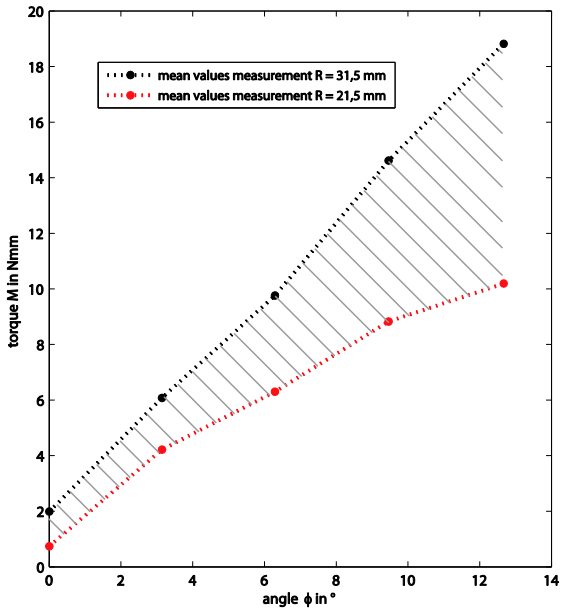

Fig 14: area of feasible angle-torque relation of JWTC 2.0 using GUTEKUNST spring with spring constant k = 0.036 N/mm

5. FUTURE WORK AND CONCLUSION

In a next step the hitherto gained results and scientific findings are used to implement the JWTC inside the underactuated swimming robot URMELE. By influencing the joint compliance the authors want to provoke changes in the locomotion pattern while the robot is swimming. Therefore this article introduced the design according to VDI 2206 of a joint with tunable compliance. Based on mathematical model and a multi-body-simulation, a first prototype of the JWTC was manufactured. In contrast to other compliant actuators ([5],[7]), the change in the angle-torque relation of the joint is provoked by changing the distance between the center line of the joint and the linear helical springs used. Comparing calculation/simulation and data gained by experiment proves the change of the angle-torque relation. Successively, a second version, the JWTC 2.0 is introduced, where the change of distance R is set by actuators.

REFERENCES

[1] Blickhan, R. (1989). The spring-mass model for running and hopping. J. Biomech. 22, pp. 1217–1227

[2] Cavagna, G. A., Heglund, N. C. & Taylor, C. R. (1977). Mechanical work in terrestrial locomotion: two basic mechanisms for minimizing energy expenditure. Am. J. Physiol. 233, pp. 243 – 261

[3] Fremerey, M., Fischheiter, F., Mämpel, J. & Witte, H. (2012). Reducing complexness of control by intelligent mechanics in undulant swimming robots, Int. J. of Design & Nature and Ecodynamics, 7(1), pp. 1 – 13

[4] Fremerey, M., Fischheiter, L., Mämpel, J. & Witte, H. (2009). Design of a single actuated, undulant swimming robot, Proceedings of 3rd International Symposium on Mobiligence, Awaji, Japan, pp. 174 – 178

[5] Hollander, K., Sugar, T., & Herring, D. (2005). Adjustable robotic tendon using a 'jack spring', in Proc. 9th Int. Conf. Rehabilitation Robotics (ICORR'05), June–July 2005, pp. 113 – 118

[6] Vanderborght, B., Van Ham, R., Lefeber, D., Sugar, T. G., & Hollander, K. W. (2009). Comparison of mechanical design and energy consumption of adaptable, passive-compliant actuators. *The International Journal of Robotics Research*, *28*(1), 90-103.

[7] Van Ham, R., Van Damme, M., Verrelst, B., Vanderborght, B., & Lefeber, D. (2007). 'MACCEPA', the mechanically adjustable compliance and controllable equilibrium position actuator: A 3DOF joint with 2 independent compliances, Int. Appl. Mech., vol. 4, pp. 130 – 142

CONTACTS

Dipl.-Ing. Max Fremerey maximilian-otto.fremerey@tu-ilmenau.de

Prof. Dipl.-Ing. Dr. med. (habil.) H. Witte hartmut.witte@tu-ilmenau.de